Performance of Nonlocal Optics When Applied to Plasmonic Nanostructures

Lorenzo Stella,*,[†,‡,∥] Pu Zhang,[§] F. J. García-Vidal,*,[§] Angel Rubio,[†,‡] and P. García-González[§,‡]
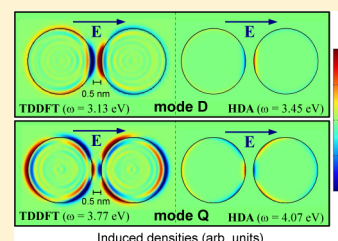
[†]Nano-Bio Spectroscopy Group, Departamento de Física de Materiales, Universidad del País Vasco, Centro de Física de Materiales CSIC-UPV/EHU-MPC and DIPC, Avenida Tolosa 72, E-20018 San Sebastián, Spain

[‡]ETSF Scientific Development Centre, Avenida Tolosa 72, E-20018 San Sebastián, Spain

[§]Departamento de Física Teórica de la Materia Condensada and Condensed Matter Physics Center (IFIMAC), Universidad Autónoma de Madrid, E-28049 Madrid, Spain

Ⓢ *Supporting Information*

ABSTRACT: Semiclassical nonlocal optics based on the hydrodynamic description of conduction electrons might be an adequate tool to study complex phenomena in the emerging field of nanoplasmonics. With the aim of confirming this idea, we obtain the local and nonlocal optical absorption spectra in a model nanoplasmonic device in which there are spatial gaps between the components at nanometric and subnanometric scales. After a comparison against time-dependent density functional calculations, we conclude that hydrodynamic nonlocal optics provides absorption spectra exhibiting qualitative agreement but not quantitative accuracy. This lack of accuracy, which is manifest even in the limit where induced electric currents are not established between the constituents of the device, is mainly due to the poor description of induced electron densities.

■ INTRODUCTION

The resonant interaction of light with metallic nanostructures is dominated by the appearance of surface plasmons. As a result, the induced electromagnetic (EM) near-field can be concentrated and enhanced in regions that are much smaller than the wavelength of the incident field.[1−3] This is the basis of a number of present and prospective applications, which include optical nanoantennas,[4] surface-enhanced Raman spectroscopy,[5,6] optoelectronics in hybrid devices,[7] optical trapping,[8] and the design of broad-band light harvesting nanostructures.[9] Therefore, there is a clear need for accurate theoretical tools able to predict optical properties of complex nanoplasmonic devices.

The main characteristics of a plasmon (frequency and lifetime) depend very sensitively on a delicate interplay between the geometrical details and the optical properties of the nanostructure.[10] Thus, time-dependent (TD) density functional theory (DFT)[11] emerges as the method of choice to perform a full quantum description of collective excitation in metals.[12] Within this framework, each electron moves independently under the action of an effective time-dependent potential which is a functional of the electron density $n(\mathbf{r},t)$. Such a functional has to account for all the many-body physics, including subtle nonlocal and memory-related effects. Fortunately, the interaction between weak EM fields and metallic nanostructures can be fairly well described through simple approximate functionals like the adiabatic local density approximation.[12−14]

However, the range of application of TD-DFT is limited by the size of the system under study. This implies that even the smallest metallic nanostructures that can be fabricated by using modern colloidal or nanolithographic synthesis techniques are far beyond the scope of TD-DFT. Then, simplified tools such as nonlocal optics based on the hydrodynamic approximation (HDA)[12,15−17] emerge as a promising way to tackle reliable analysis of realistic nanoplasmonic devices. Since the experimental realization of nanostructures exhibiting inhomogeneities at the nanometric and subnanometric scales is now possible,[18−20] it is of major importance to carry out a critical and painstaking assessment of the HDA. This is the objective of the present article.

The article is organized as follows: After a brief summary of the HDA, we will present a detailed study of the optical absorption spectrum of a model metallic nanowire. This analysis will show some of the deficiencies of local and nonlocal optics, which will be more evident when studying the optical response of a simple nanoplasmonic device made up by two metallic nanowires. To illustrate the importance of a proper treatment of the equilibrium electron density in a metal–vacuum interface, we will present some results for the so-called infinite barrier model, where the electrons within a nanostructure are confined by an infinite potential well. The corresponding conclusions will close the article.

■ THE HYDRODYNAMIC APPROXIMATION

The hydrodynamic description of the conduction electrons of a metal is given in terms of a velocity field $\mathbf{v}(\mathbf{r},t)$ and the local electron density $n(\mathbf{r},t) = n(\mathbf{r}) + \delta n(\mathbf{r},t)$, where $\delta n(\mathbf{r},t)$ is the

induced density by an external source and $n(\mathbf{r})$ is the electron equilibrium density, i.e., in the absence of external fields. In customary applications of the HDA such an equilibrium density is greatly simplified, in such a way that $n(\mathbf{r}) \simeq 0$ outside the metal and $n(\mathbf{r}) \simeq \bar{n}$ inside, $\bar{n}$ being the mean density of conduction electrons. In this case, the evolution under weak EM fields is determined by the linearized Navier−Stokes equation (e and m_e are the electron charge and mass, respectively)

$$\frac{\partial \mathbf{v}(\mathbf{r}, t)}{\partial t} = -\gamma \mathbf{v}(\mathbf{r}, t) + \frac{e}{m_e}\mathbf{E}(\mathbf{r}, t) + \frac{\beta^2}{\bar{n}}\nabla[\delta n(\mathbf{r}, t)]$$

(1)

Here, $\mathbf{E}$ is the total electric field (external plus induced), γ accounts for damping processes, and β is a characteristic velocity of the electrons in the metal. The latter just appears in the nonlocal term on the right-hand side of eq 1, i.e., the one containing the gradient of the induced density. The hydrodynamic eq 1 together with Maxwell's equations defines a self-consistent problem that can be solved analytically for selected geometries and numerically by using, for instance, finite-element methods.[12,18,21−27]

The HDA dispersion relation for longitudinal bulk plasmons is $\omega^2 = \omega_P^2 + \beta^2 k^2$, where $\omega_P = (4\pi e^2 \bar{n}/m_e)^{1/2}$ is the bulk plasma frequency.[28] Therefore, the velocity β quantifies the dispersion in the EM response. This issue becomes important when the distances between metallic objects and/or their radii of curvature are less than a few nanometers, which is the limit where the local optics prescription ($\beta = 0$) is expected to break down.[9,18,19,29] The usual choice in nonlocal optics applications is $\beta = (3/5)^{1/2}v_F$, where $v_F = (3\pi^2 \bar{n})^{1/3}\hbar/m_e$ is the Fermi velocity of the conduction electrons.[28] This value of β reproduces fairly well the dispersion relation of bulk plasmons and, therefore, is suitable for the description of those high-frequency phenomena that mainly induce compressions/expansions of the electron fluid. Nonetheless, the nature of confined surface plasmons that occurs in metallic nanostructures is closer to collective displacements of the electron fluid rather than to a longitudinal pressure wave. For this kind of phenomenon it is then more appropriate to derive the nonlocal dispersion term by considering the variation of the electron gas energy under quasi-static perturbations.[30] The expression for β should be instead[16,17]

$$\beta = \left[\frac{1}{3}v_F^2 + \frac{\bar{n}}{m_e}\frac{\partial^2 e_{XC}(\bar{n})}{\partial \bar{n}^2}\right]^{1/2}$$

(2)

with $e_{XC}(\bar{n})$ being the exchange-correlation energy per volume of a homogeneous electron gas of density $\bar{n}$. Under this perspective, the HDA can be seen as an orbital-free and quasi-static approximation to TD-DFT but still accounting by construction for some important quantum effects, like Pauli's exclusion principle. However, the HDA neglects the existence of electron−hole excitations, and the quantum nature of a plasmon (which is nothing but a set of coherent electron−hole excitations) is oversimplified.

As mentioned, typical applications of local and nonlocal optics consider neither the ionic structure of the metals nor the electron density spill-out at the metal−vacuum interface. The former is a legitimate approximation for clean simple sp metal interfaces, and the so-called jellium model can be safely used even under the quantum description of the collective response of the electrons.[31] Moreover, the screening due to d-electrons

in noble metals[32,33] and/or the presence of dielectric overlayers[34] can be easily incorporated into the jellium model without sacrificing its simplicity. On the contrary, a proper treatment of the electron density spill-out is mandatory for a detailed understanding of the collective excitations at metal surfaces.[31]

■ OPTICAL SPECTRUM OF A SINGLE SODIUM NANOWIRE

To critically assess the capabilities of the semiclassical HDA and identify its limits, let us start with a simple test case: a jellium sodium nanowire of circular section. This metallic cylinder is irradiated by light whose propagation direction and E-field polarization lie on the plane perpendicular to the direction Z of the nanowire axis. As a consequence, the system behaves as a two-dimensional one in the linear response limit. We have chosen a radius $R = 2$ nm, which is large enough to accommodate collective excitations. It must be noted that the application of the HDA to narrower structures makes no sense since single electron−hole optical transitions cannot merge into well-defined plasmon peaks.[35] For sodium we have that $\bar{n} = 25.173$ nm^{-3} and $\omega_P = 5.891$ eV, whereas $\beta = 0.31 \times 10^6$ m/s (note that the customary value of the β-velocity, $(3/5)^{1/2}v_F$, is equal to 0.82×10^6 m/s). Finally, since damping processes in this system are mainly due to the scattering of moving electrons by the barrier potential at the cylinder surface, γ must be of the order of $\hbar v_F/R \sim 0.3$ eV.[36]

The sets of differential equations for classical local and semiclassical nonlocal HDA optics are solved numerically using the finite element COMSOL package[37] following the prescription by Raza et al.[25,38] and Hiremath et al.[39] Unlike it was done in some previous applications of the HDA to nanowires,[22,23] such an implementation does not neglect the transverse component of the induced electric field. It is known that this simplification enforces the definition of additional but artificial boundary conditions to obtain a unique solution of the HDA problem, which results in the appearance of spurious resonances in the absorption spectrum.[25] Regarding the quantum simulations, we use the Octopus package in which the TD-DFT equations are solved in real space and time domains.[40−42] We have implemented the translational symmetry of the nanowires in Octopus for both static (ground state) and time-dependent calculations by imposing periodic Born−von Kármán boundary conditions on the Z direction (no supercell is defined on the XY plane since Octopus is a real-space code).

The main results for the single nanowire are presented in Figure 1. The TD-DFT absorption spectrum is dominated by a main confined surface plasmon at $\omega = 4.09$ eV, which is slightly red-shifted with respect to the classical value $\omega_{SP} = \omega_P/\sqrt{2} = 4.17$ eV. This feature is well-known in metallic nanoparticles[43,44] and arises because the induced density moves outside the geometrical boundaries of the object, thus slowing the oscillation of the collective mode. However, upon inspection of the externally driven induced electron density (see the panel b of Figure 1), one can realize that this resonance is not a pure surface mode as it also contains a distinctive contribution from the center of the nanowire. Hence, the main peak is actually the superposition of a surface plasmon plus a collective dipole excitation localized around the center of the nanowire. These modes, coined as quantum core (QC) plasmons, have been recently predicted by TD-DFT calculations of the absorption spectra of metallic nanospheres.[44]
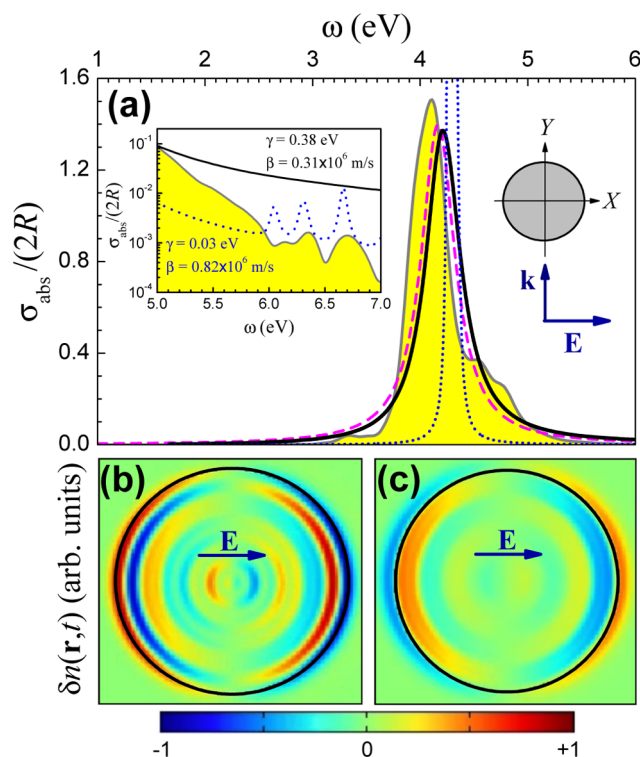
Figure 1. (a) Normalized absorption cross section per unit length, σ_{abs}, for a jellium sodium nanowire of radius $R = 2$ nm. Solid line with filled area: TD-DFT; solid line: HDA ($\beta = 0.31 \times 10^6$ m/s, $\gamma = 0.38$ eV); dashed line: local optics ($\gamma = 0.38$ eV); dotted line: HDA ($\beta = 0.82 \times 10^6$ m/s, $\gamma = 0.03$ eV). The inset shows in logarithmic scale the behavior of the optical absorption in the region around the bulk plasmon frequency ($\omega_P = 5.89$ eV). (b) Snapshot of the TD-DFT driven induced density (in arbitrary units) by a short "sinusoidal" electromagnetic pulse (see Supporting Information) of frequency $\omega = 4.09$ eV at $t = 7.25T$ (T is the period of the incident field). (c) Same as panel b but for an external field of frequency $\omega = 4.60$ eV at $t = 6.25T$.

Since this spectral feature is related to a strong quantum confinement, we expect to observe such modes in metallic nanowires.
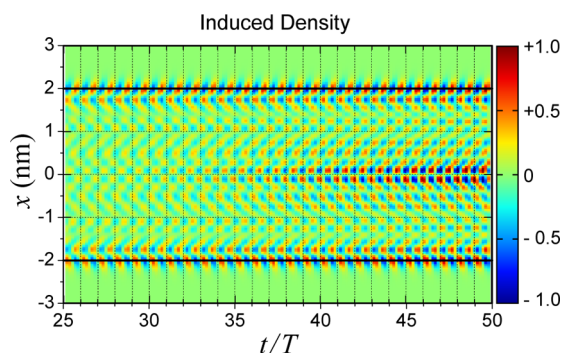

Figure 2. TD-DFT induced density (in arbitrary units) along the transverse axis, i.e., parallel to the incident electric field, of an isolated nanowire. The density response is driven by a "trapezoidal" pulse (see text), and the time is measured in number of cycles (the period of the incident field is $T \approx 1$ fs). Note that the reported evolution is restricted to the central interval of the external pulse. The signature of the QC plasmon clearly appears at $t \approx 35T$.

With the aim of confirming this idea, in Figure 2 we report the TD-DFT induced density of an isolated nanowire of radius 2 nm driven by the electromagnetic external perturbation

$$\mathbf{E}(r, t) = -E_0 \cos(\omega t)\mathbf{u}_x \begin{cases} t/t_1 & 0 \leq t < t_1 \\ 1 & t_1 \leq t < t_2 \\ (t_{fin} - t)/(t_{fin} - t_2) & t_2 \leq t < t_{fin} \end{cases} \quad (3)$$

where $t_1 = t_2 - t_1 = t_{fin} - t_2 = 26.34$ fs. The shape of the pulse has been chosen to mimic the adiabatic onset of an almost plane wave of angular frequency $\omega = 4.1$ eV ($T = 2\pi/\omega \approx 1$ fs), i.e., the resonant frequency of the main surface plasmon of the nanowire. Also note that this pulse is much longer than the one used to evaluate the TD-DFT induced densities depicted in Figure 1. The QC plasmon clearly appears after 35 fs as a dipole-like oscillation localized at the center of the nanowire.

A second weaker spectral feature appears in the TD-DFT spectrum around $\omega = 4.6$ eV, and a snapshot of the corresponding driven induced density is displayed in the panel c of Figure 1. This is another surface excitation that may be identified as a Bennet multipole surface plasmon.[45] This mode is intimately related to the electron spill-out at the edge of the nanostructure, and its charge distribution along the direction perpendicular to the surface has a predominant dipole shape (the corresponding distribution of the standard surface plasmon is mainly monopole). Nevertheless, that monopole or dipole character is partially lost for driven modes like the ones depicted in Figure 1, and it only applies rigorously to the eigenmodes of the inverse dielectric function at complex resonant frequencies.[46]

There are some other tiny structures that can be attributed to individual electron–hole excitations or to less intense QC plasmons. Finally, as is shown in the inset of Figure 1, a series of extremely weak but well-defined excitations appear above the bulk plasma frequency ω_P. These are Landau damped confined longitudinal bulk plasmons, whose existence in metallic nanowires was first conjectured by Ruppin[21] and detected experimentally in thin metal films several decades ago.[47]

Let us now analyze the results given by local optics and the semiclassical HDA. As is very well-known, the local-optics absorption spectrum consists of a single peak centered at ω_{SP} without further spectral features. This resonance is slightly blue-shifted to $\omega = 4.21$ eV when nonlocal effects are included via the HDA. The widths of these peaks depend on the value of γ. By choosing $\gamma = 0.38$ eV, we see that the overall shape of both local and HDA resonances are in good agreement with the TD-DFT one. Note that this value is fully consistent with our initial guess $\gamma \sim 0.3$ eV. We must emphasize that the slightly better performance of local optics is simply due to a cancellation of errors. Namely, local optics neglects the equilibrium density spill-out (which leads to a red-shift of the main plasmon peak with respect to the value ω_{SP}) *and* nonlocal response features (whose inclusion is reflected, as we have just mentioned, by a blue-shift of the main absorption peak). The HDA corrects the latter deficiency but not the former.

On the other hand, Bennet multipole plasmon appears neither in the local nor in the HDA spectra also due to the absence of spill-out for the electrons. Finally, in the HDA spectrum, the use of a relatively large damping prevents from the appearance of the series of confined bulk plasmons above ω_P. However, the HDA reproduces fairly well the positions of such resonances but using $\beta = 0.82 \times 10^6$ m/s and $\gamma = 0.03$ eV, that is, the values amenable for describing longitudinal bulk

density waves. Note that these modes also appear if $\beta = 0.31 \times 10^6$ m/s, although slightly blue-shifted. In any case, these subsidiary resonances do not play any role in actual plasmonic devices. Besides, the surface plasmon frequency corresponding to $\beta = 0.82 \times 10^6$ m/s is too large ($\omega = 4.31$ eV), as it can be observed in Figure 1. Hence, we will take hereafter $\gamma = 0.38$ eV and $\beta = 0.31 \times 10^6$ m/s as HDA parameters.

■ NANOWIRE DIMERS

A much more stringent playground for nonlocal optics is a plasmonic nanostructure made up by two parallel sodium nanowires. The one-dimensional extension of this system enhances the short-range electrostatic coupling between nanowires, which is maximum when the electric field is directed along the dimer axis, X. Therefore, this is a harder test for the HDA than nanoparticle dimers, whose classical and quantum responses have been extensively investigated in the last years.[2,20,26,48−51] We will then concentrate on the response against an electric field parallel to the dimer axis, whereas the analysis for polarized light in the perpendicular direction, Y, will be briefly discussed in the subsequent section.

The TD-DFT absorption spectra versus the spatial gap d between cylinders is presented in panel a of Figure 3. In fair correspondence with the quantum response of nanosphere dimers,[49−51] we can distinguish three regimes. At large distances ($d \geq 1.5$ nm), the main plasmon peak red-shifts and broadens when decreasing the separation between the nanowires. At intermediate distances (0.5 nm $\leq d < 1.5$ nm)

this peak splits in two. Finally, at short distances ($d < 0.5$ nm) the absorption spectra changes drastically due to the possibility of charge transfer between the nanowires: the lower energy mode suddenly vanishes, and new spectral features emerge.

The main behavior at long and intermediate distances is the result of a hybridization of the surface modes of the two nanowires,[52] in such a way that the lower [higher] energy resonance corresponds to a mode with overall dipole (D) [quadrupole (Q)] character. Bennet surface modes (M) are not affected by this hybridization, which explains the presence of the resonance at $\omega = 4.6$ eV for all the geometries here considered. Interestingly, the quadrupole resonance seems to be more intense than the dipole one at intermediate distances, which is the opposite trend that the hybridization model predicts and that has been indeed calculated for nanosphere dimers.[49−51]

We attribute this distinct behavior to the mixed character of the surface plasmon of a single cylinder. The hybridization between QC plasmons is very weak since they are concentrated deeply into the nanowires, and when they approach each other, the D and Q surface resonances red-shift but not the QC plasmons. As a consequence, the QC plasmons can be now identified in the absorption spectra (indicated by arrows in Figure 3) while still contributing to the weight of the Q peaks. This feature is illustrated in Figure 4, where we show the

Figure 4. Numerical decomposition of the TD-DFT absorption spectrum of two nanowires of radius 2 nm, separated by a distance of 0.5 nm. The contributions from the quadrupole (Q) and QC plasmons are indicated along with the Bennet multipole (M) plasmon.

numerical (Gaussian) decomposition of the main TD-DFT absorption peak of two nanowires at intermediate distance ($d = 0.5$ nm). In this case, the superposition of the quadrupole (Q) and QC plasmon lines is still substantial, but not complete. Indeed, the Q mode appears at $\omega = 3.75$ eV, whereas the QC plasmon resonant frequency is $\omega = 4.02$ eV. Hence, the QC plasmon is unveiled in the spectrum while keeping an enhancement of the response for $\omega \approx 3.8$ eV. The presence of the QC plasmon is also evident when observing the induced density driven by the perturbation (3) with $\omega = 4.02$ eV. In Figure 5 we display such induced density along the dimer axis, X. The QC plasmon is fully developed at $t \simeq 35$ fs, although there is a clear signature just after the adiabatic switching of the external field at $t \simeq 26$ fs. On the contrary, the near Q mode is not well-defined since there is no induced density in the nanowire junction (a signature of such a mode, as we will see later on). Although not the main point of this article, these results support the idea[44] that the QC plasmon can strongly
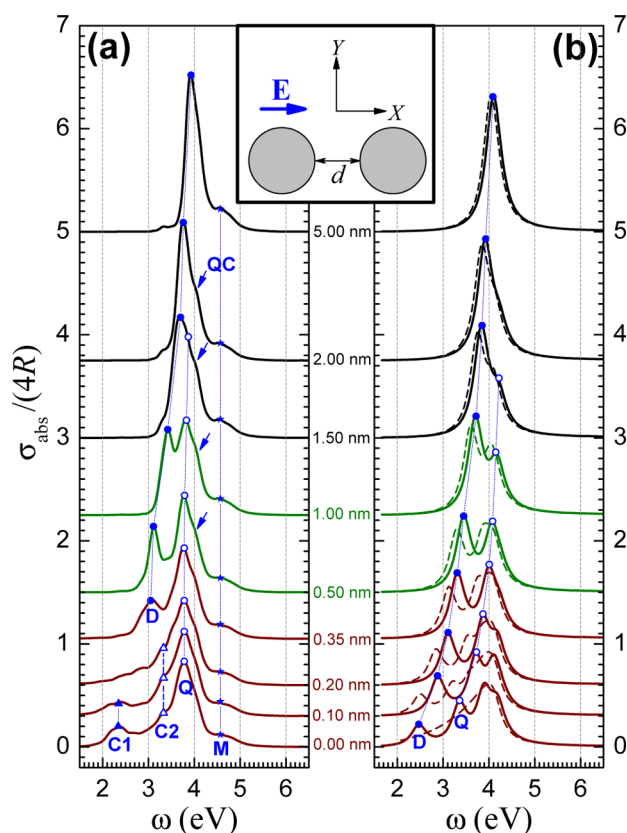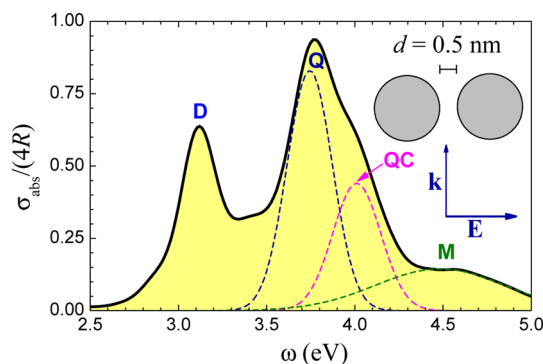
Figure 3. Waterfall representation of the normalized absorption cross section per unit length for a sodium nanowire dimer versus the distance d. (a) TD-DFT. (b) HDA (solid lines) and local optics (dashed lines).
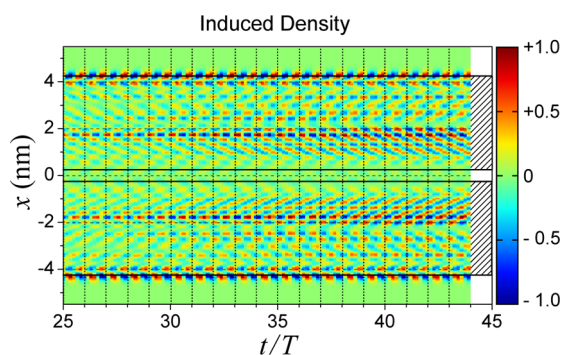
Figure 5. TD-DFT induced density (in arbitrary units) along the transverse axis, X, of a nanowire dimer ($d = 0.5$ nm). The density response is driven by a "trapezoidal" pulse of frequency $\omega = 4.02$ eV (the corresponding period is $T = 1.03$ fs). The extension of the jellium background is sketched in the right part of the figure.

effect the linear spectra of metallic nanostructures, even for extend geometries, e.g., nanowires.

Local optics and the HDA account qualitatively well for the hybridization process (see the right panel of Figure 3). At large distances, the overall small blue-shift in the spectra is just the concomitant consequence of the lack of electron density spill-out in each nanowire. However, at intermediate distances the quantitative discrepancies are more serious. First of all, since these orbital-free prescriptions are not able to describe QC plasmons, the Q peak is always less intense than the D one. Second, although the local-optics spectrum remains closer to the TD-DFT one, it overestimates the hybridization (a third hybridized mode begins to emerge at $d = 0.5$ nm). Finally, the HDA performance is apparently poorer than the local-optics one. This is an unexpected result since this is precisely the limit where the HDA should supersede the standard local-optics approach. All these features are shown in Figure 6, where we have also included the HDA spectrum using $\beta = (3/5)^{1/2} v_F$. As we may see, this choice worsens the accuracy of the HDA even more.

As anticipated in the previous section, the ultimate reason for the quantitative failure of the HDA is the inaccurate description of the induced densities that appear on each cylinder surface. As it may be observed in panels b and c of Figure 6, the TD-DFT induced density spreads into the vacuum in such a way that the effective location of the surface is outside the jellium background edge. On the contrary, albeit showing the right dipole or quadrupole symmetry, the HDA induced densities remain within the limits of the jellium background due to the use of a stepped ground-state density profile: the effective location of the surface is inside the jellium edge. Finally, the induced densities under the local approximation are strictly confined on the jellium edge, which is then the effective surface. As a consequence, the HDA underestimates the interaction between induced densities and the hybridization itself, but the underestimate is less severe when using local optics. However, the latter is achieved thanks to an unphysical description of the induced density. Note that a direct comparison between HDA and local optics spectra serves to estimate the importance of nonlocality in the response to the external EM field. Hence, we conclude that in the limit of nanometric and subnanometric spatial gaps the inhomogeneity of the density profile at a surface can be more important than the nonlocality of that EM response. Finally, the relative penetration of the electron density into the gap between the nanostructures depends
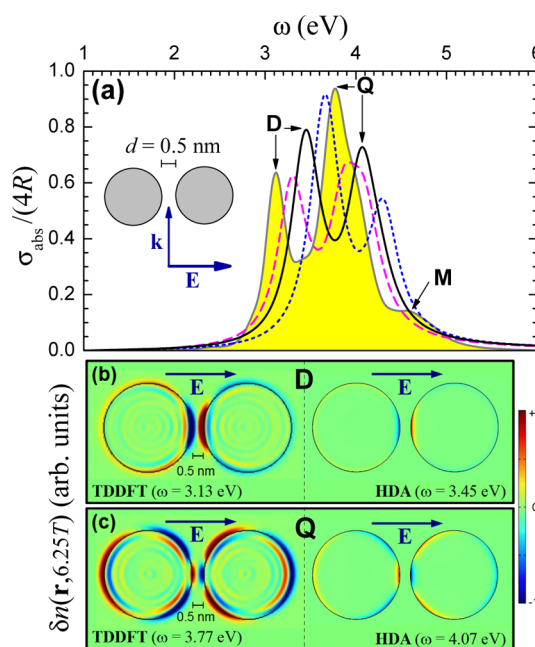

Figure 6. (a) Optical absorption spectrum of a sodium nanowire dimer ($R = 2$ nm, $d = 0.5$ nm). Solid line with filled area: TD-DFT; solid line: HDA ($\beta = 0.31 \times 10^6$ m/s); dashed line: local optics; dotted line: HDA ($\beta = 0.82 \times 10^6$ m/s). The local-optics and HDA calculations have been performed with a damping frequency $\gamma = 0.38$ eV. (b, c) TD-DFT (snapshot at $t = 6.25T$) and HDA driven densities (in arbitrary units) corresponding to the hybridized dipole plasmon (D) and the quadrupole one (Q), respectively. The induced densities given by the local approach are singular since they are purely surface densities and, consequently, are not presented.

primarily on the distance d, but not on the size of the nanostructures. As a consequence, the discrepancies between HDA and TD-DFT findings are also expected to appear for larger plasmonic nanostructures with subnanometric gaps.

A technological interest behind the development of plasmonic nanostructures is the concentration of the electromagnetic field in spacial regions smaller than the wavelength of the incident radiation. Therefore, although the study of the induced densities and the absorption spectra is already suitable to assess the quality of the local and nonlocal optics prescriptions, the analysis of the near-field electric response is appealing for practical plasmonic applications. In the dimer case, due to the resonant interaction between the nanowires, the electric field should exhibit a pronounced enhancement in the near-field as long as the overlap between the electron densities of the two wires is negligible.

Focusing on the case of $d = 0.5$ nm (see Figure 7), for the dipole hybridized mode (D) a substantial electric field enhancement is observed in the gap region by means of all the three methods considered in this article. However, TD-DFT predicts an electric field enhancement in a region which is slightly narrower than the one predicted by both the local and HDA prescriptions. On the other hand, the TD-DFT enhancement is maximum just in the center of the gap, whereas the HDA and local optics predict that such maximum is reached on the surface of the metallic nanostructures. These discrepancies can be easily interpreted as a consequence of the proper treatment of the electron density spill-out in the TD-DFT and are consistent with the recent results of Zuloaga and co-workers about the field enhancement of jellium nanosphere
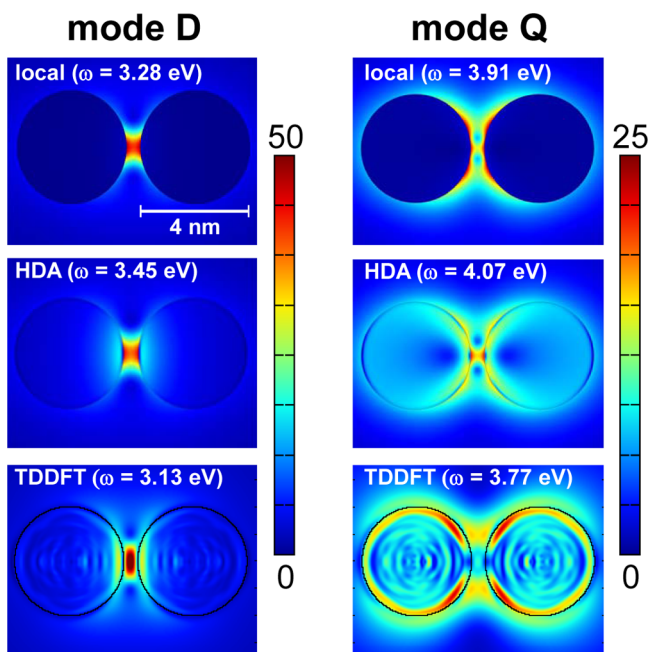
Figure 7. Electric field enhancement $|\mathbf{E}_{tot}(\mathbf{r})|/|\mathbf{E}_{in}|$ corresponding to the dipole (D) and quadrupole (Q) hybridized modes of a sodium nanowire dimer ($d = 0.5$ nm). Top panels: local optics; middle panels: HDA; lower panels: TD-DFT. The induced fields have been evaluated at the resonant frequencies indicated in the panels.

dimers.[49] However, the situation is completely different when the electric field induced by the quadrupole hybridized mode (Q) is considered. First of all, there are already substantial differences between the local and the hydrodynamic approaches. However, none of these approximations is able to reproduce the electric field enhancement given by the TD-DFT benchmark calculation. In particular, the intensity of the TD-DFT induced field reaches its maximum in the surface region next to the gap—not in the gap itself—while it is non-negligible in a broad region around the whole nanostructure. On the other hand, this lack of agreement for the Q mode looks less surprising bearing in mind the quantitative differences between the HDA and TD-DFT induced electron densities discussed above.

Finally, let us discuss the short-distance limit ($d < 0.5$ nm). In this regime the ground-state density profiles of the nanowires overlap, and they cannot be considered as individual entities anymore. Consequently, the incident light can induce an electric current across the dimer junction, which changes the response substantially. As is shown in Figure 3, the dipole plasmon dramatically loses spectral weight and actually vanishes for $d < 0.3$ nm, the frequency of the quadrupole mode remains practically constant, and two new modes (charge transfer plasmons) appear.[48,50,51] It is worth noting that the first of these resonances, C1, is more intense than its counterpart in nanosphere dimers. Obviously, the reason is that the relative extension of the density superposition is now larger than in nanoparticle dimers. On the other hand, the transfer of spectral weight from the hybridized quadrupole plasmon to the second charge transfer plasmon, C2, is partially hidden by the ubiquitous presence of the QC plasmon at $\omega \simeq 4.0$ eV.

Local and HDA optics in the present implementation are not expected to be accurate at all in this regime. Any resemblance between their spectra and the TD-DFT one is merely

coincidental, since the physical mechanisms that lead to the resonances are completely different in each case. For instance, the attenuation of the hybridized dipole plasmon predicted by local optics is an artifact of the local approach itself,[27] and the peak that appears at 2.46 eV in the HDA absorption spectrum for touching geometry has nothing to do with the TD-DFT resonance at 2.39 eV: the latter is a charge transfer mode while the former is a hybridized dipole plasmon (see Figure 3).

The importance of charge-transfer processes in the excitation spectra of nanoparticle dimers is well recognized and can be measured experimentally.[20] Keeping the simplicity of classical local and semiclassical nonlocal optics, such processes can be modeled by including either a metallic neck[48] or a dielectric medium[51,53] across the dimer junction. The modification of the spectrum given by the first solution, where the width of the neck has been determined by inspection of the DFT ground-state density, is depicted in Figure 8 for touching cylinders ($d =$
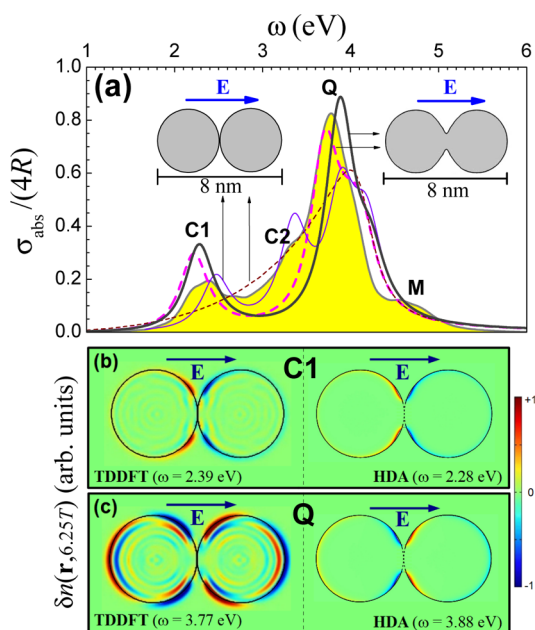

Figure 8. (a) Absorption spectrum of a sodium nanowire dimer ($R = 2$ nm) at touching geometry. Filled solid line: TD-DFT; thick solid and dashed lines: HDA and local optics, respectively, with a geometry accounting for charge transfer; thin solid and dashed lines: HDA and local optics, respectively, with a singular contact between the nanowires. (b, c) Driven induced densities (in arbitrary units) corresponding to the first charge transfer plasmon (C1) and the bonding quadrupole plasmon (Q), respectively, under the TD-DFT and HDA prescriptions.

0). Local optics and the HDA reproduce the main spectral features except the shoulder due to C2 mode. The overall qualitative agreement is remarkable if one bears in mind the oversimplified description of the dimer bonding. Nevertheless, we found that the intensity and position of the charge transfer plasmon in this model depend quite sensitively on the width and shape of the metallic neck.

■ THE *E*-FIELD POLARIZATION PERPENDICULAR TO THE DIMER AXIS

For the sake of completeness, we depict in Figure 9 the optical absorption spectra of nanowire dimers corresponding to an incident electric field polarized along the direction perpendic-
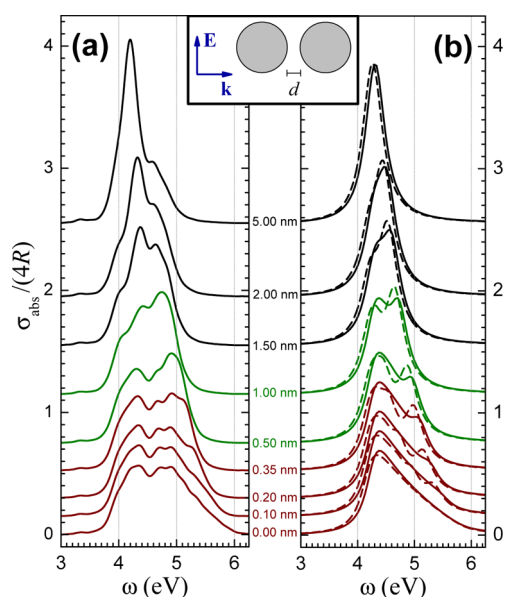
Figure 9. Waterfall representation of the normalized (by 4 times the nanowire radius, R) absorption cross section per unit length for nanowire dimers when the E-field polarization is perpendicular to the dimer axis (see inset). (a) TD-DFT. (b) HDA (solid lines) and local optics (dashed lines).

ular to the dimer axis. In this case, the discrepancies between the TD-DFT and the semiclassical hydrodynamic approximation (HDA) are not as serious as the ones arising when the E-field is parallel to the dimer axis. Moreover, the HDA correction to the local optics results is less evident.

As it can be seen in the left panel of Figure 9, the dominant mechanism here is the hybridization of the surface modes of the two nanowires.[52] At large distances ($d \geq 1.5$ nm), the main surface plasmon peak slightly blue-shifts and broadens when the distance between the nanowires is decreased (note that the small peak at $\omega \approx 4.6$ eV for $d = 1.5$ nm has a strong contribution from the Bennet multipole surface plasmons at each nanowire). For shorter distances, the main peak splits in two: a well-defined resonance appears at $\omega \approx 4.3$ eV, whereas the original peak blue-shifts and loses spectral weight very quickly. That new resonance and the QC plasmon at $\omega \approx 4.0$ eV partially overlap. Finally, in the regime where there is a covalent bond between the nanowires ($d \leq 0.35$ nm), a weak spectral feature emerges at $\omega \approx 4.9$ eV. However, since the external electric field is perpendicular to the dimer axis, there is not charge transfer between the nanowires. The HDA and local optics prescriptions describe this process rather well. In fact, the main discrepancies are the absence of QC and Bennet plasmons and, to a lesser extent, the overestimated spectral transfer between hybridized modes at intermediate distances.

■ THE INFINITE BARRIER MODEL

To illustrate the relevance of the equilibrium density profile $n(\mathbf{r})$, we have performed some TD-DFT calculations imposing an external potential which strictly confines the electronic density within the geometrical limits of the jellium background. This is the so-called infinite barrier model (IBM).

The effect of this rather unphysical constraint can be observed by comparing the absorption cross sections of an isolated nanowire obtained by the TD-DFT/IBM approximation against different numerical approaches, as shown in Figure

10. First of all, the whole TD-DFT/IBM absorption spectrum is dramatically blue-shifted—the main surface plasmon resonance
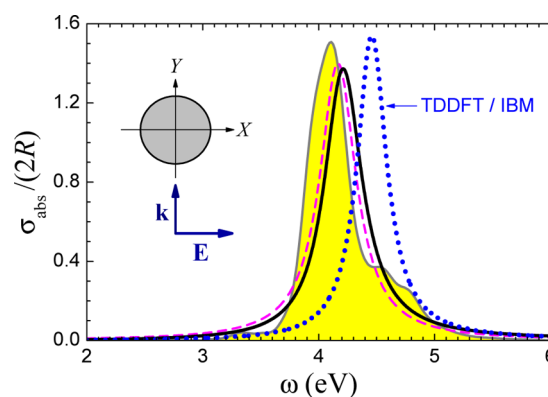

Figure 10. Normalized absorption cross section per unit length, σ_{abs}, for a jellium sodium nanowire of radius $R = 2$ nm. Solid line with filled area: standard TD-DFT; solid line: HDA ($\beta = 0.31 \times 10^6$ m/s, $\gamma = 0.38$ eV); dashed line: local optics ($\gamma = 0.38$ eV); dots: TD-DFT but using the infinite barrier model to describe the confinement of the electrons.

occurs at $\omega \sim 4.45$ eV—since the conduction electrons are overconfined by the IBM. In particular, the TD-DFT/IBM electron density (not shown) is identically zero outside the background region, but it does not show a sharp edge as the HDA equilibrium density does. Indeed, the TD-DFT/IBM electronic density quickly, yet smoothly, goes to zero across a finite region close to surface. This behavior gives a confinement effectively stronger than for the HDA and then a larger blue-shift in the absorption cross section. Therefore, it is not surprising that the main peak of the HDA spectrum lies between the main peak of benchmark TD-DFT calculation (built upon an electron density that spills out the jellium edge) and the main peak of the TD-DFT/IBM one (built upon an electron density effectively overconfined).

A second interesting feature appearing in Figure 10 is the absence of the multipole Bennet plasmon in the TD-DFT/IBM spectrum. This result can be easily interpreted in terms of the increased stiffness of the electron density within the TD-DFT/IBM approximation.[31] Finally, although not presented in Figure 10, the longitudinal confined bulk plasmons can be still observed in the TD-DFT/IBM spectrum. This spectral feature is expected since the overconfinement acts in a finite region very close to the jellium surface, while the bulk electron density remains unchanged.

Taking into account the results for a single nanowire, it is fairly easy to interpret the absorption spectrum of a nanowire dimers within the TD-DFT/IBM approximation. Apart from an overall blue-shift of the whole spectrum due to the over-confinement, the plasmon hybridization process will be less efficient owing to the absence of the electron density spill-out. Indeed, in Figure 11—in which we present the absorption spectrum for a nanowire dimer ($d = 0.5$ nm)—one can observe that the heights and positions of the two HDA main peaks are between the corresponding values of the TD-DFT and TD-DFT/IBM approximations. This final result further supports the main conclusions of the article, i.e., the extreme sensitivity to the equilibrium electronic density profile of the plasmonic response of metallic nanostructure showing nanometric and subnanometric features such as dielectric gaps.
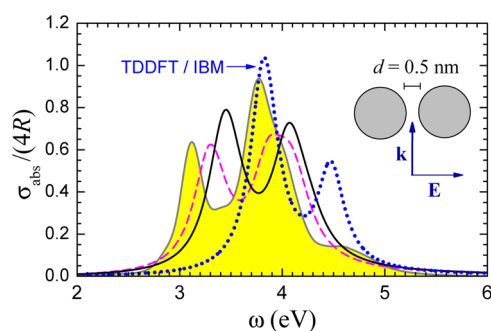
Figure 11. Optical absorption spectrum of a sodium nanowire dimer ($R = 2$ nm, $d = 0.5$ nm). Solid line with filled area: standard TD-DFT; solid line: HDA ($\beta = 0.31 \times 10^6$ m/s, $\gamma = 0.38$ eV); dashed line: local optics ($\gamma = 0.38$ eV); dots: TD-DFT but using the infinite barrier model to describe the confinement of the electrons.

CONCLUSIONS

Albeit the merits of the HDA analysis of some nanoplasmonic experiments cannot be disregarded,[18,19] our work seeds serious doubts about the overall accuracy of standard HDA. This lack of accuracy has been demonstrated for sodium nanowires whose separation is of the order of the electron spill-out, i.e., even when the conduction contact between the wires is not reached yet. Being the electron spill-out a feature of all metallic surfaces, we also expect a similar lack of accuracy of standard HDA when applied to noble metals. In each case, all the length scales must be rescaled according to the spill-out of the metal under consideration, and some correction to the bare jellium model can be applied.[32−34] For larger objects, it is very likely that QC plasmons will have a minor impact in the optical spectrum. However, we expect that the details of the interaction between induced densities around nanometric gaps will be crucial regardless the size of the components. Since the distribution of the induced density and the corresponding E-field enhancement depend very much on the details of the equilibrium density,[54] this must be accounted for in future implementations of the HDA. In addition, as we have clearly shown in this article, both the nonlocal response and the equilibrium density spill-out must be treated on the same footing to obtain accurate numerical predictions. However, the straightforward inclusion of inhomogeneous density profiles into the HDA is not entirely robust and has some fundamental problems.[55] Henceforth, nontrivial modifications of the HDA and/or divide-and-conquer strategies which combine nonlocal semiclassical optics and TD-DFT methods are still needed in the emerging field of quantum nanoplasmonics. The latter will also pave the way for an atomistic description of metal interfaces of nanoplasmonic devices. Work along these lines are in the horizon.

ASSOCIATED CONTENT

ⓢ Supporting Information

Three movies showing the evolution of the driven induced density corresponding to the D and Q modes ($d = 0.5$ nm) and to the C1 mode ($d = 0$). This material is available free of charge via the Internet at http://pubs.acs.org.

AUTHOR INFORMATION

Corresponding Author

*E-mail: lorenzo.stella@ehu.es (L.S.); fj.garcia@uam.es (F.J.G.-V.).

Present Address

‖Department of Physics, School of Natural and Mathematical Sciences, King's College London, The Strand, London WC2R 2LS, UK.

Notes

The authors declare no competing financial interest.

REFERENCES

(1) Maier, S. A. *Plasmonics: Fundamentals and Applications*; Springer: New York, 2007.

(2) Halas, N. J.; Lal, S.; Chang, W.-S.; Link, S.; Nordlander, P. Plasmons in Strongly Coupled Metallic Nanostructures. *Chem. Rev.* **2011**, *111*, 3913−3961.

(3) Gray, S. K. Theory and Modeling of Plasmonic Structures. *J. Phys. Chem. C* **2013**, *117*, 1983−1994.

(4) Mühlsclegel, P.; Eisler, H.-J.; Martn, O. J. F.; Hecht, B.; Pohl, D. W. Resonant Optical Antennas. *Science* **2005**, *398*, 1607−1609.

(5) Xu, H.; Bjeneld, E.; Käll, M.; Börjesson, L. Spectroscopy of Single Hemoglobin Molecules by Surface Enhanced Raman Scattering. *Phys. Rev. Lett.* **1999**, *83*, 4357−4360.

(6) Vo-Dinh, T.; Dhawan, A.; Norton, S. J.; Khoury, G. K.; Wang, H.-N.; Misra, V.; Gerhold, M. D. Plasmonic Nanoparticles and Nanowires: Design, Fabrication and Application in Sensing. *J. Phys. Chem. C* **2010**, *114*, 7480−7488.

(7) Ward, D. R.; Hüser, F.; Pauly, F.; Cuevas, J. C.; Natelson, D. Optical Rectification and Field Enhancement in a Plasmonic Nanogap. *Nat. Nanotechnol.* **2010**, *5*, 732−736.

(8) Tsuboi, Y.; Shoji, T.; Kitamura, N.; Takase, M.; Murakoshi, K.; Mizumoto, Y.; Ishihara, H. Optical Trapping of Quantum Dots Based on Gap-Mode-Excitation of Localized Surface Plasmon. *J. Phys. Chem. Lett.* **2010**, *1*, 2327−2333.

(9) Aubry, A.; Lei, D. Y.; Fernández-Domnguez, A. I.; Sonnefraud, Y.; Maier, S. A.; Pendry, J. B. Plasmonic Light-Harvesting Devices over the Whole Visible Spectrum. *Nano Lett.* **2010**, *10*, 2574−2579.

(10) Stender, A. S.; Wang, G.; Sun, W.; Fang, N. Influence of Gold Nanorod Geometry on Optical Response. *ACS Nano* **2010**, *4*, 7667−7675.

(11) Runge, E.; Gross, E. K. U. Density-Functional Theory for Time-Dependent Systems. *Phys. Rev. Lett.* **1984**, *52*, 997−1000.

(12) Pitarke, J. M.; Silkin, V. M.; Chulkov, E. V.; Echenique, P. M. Theory of Surface Plasmons and Surface-Plasmon Polaritons. *Rep. Prog. Phys.* **2007**, *70*, 1−87.

(13) Onida, G.; Reining, L.; Rubio, A. Electronic Excitations: Density-Functional Versus Many-Body Green's-Function Approaches. *Rev. Mod. Phys.* **2002**, *74*, 601−659.

(14) Marques, M. A. L., Maitra, N. T., Nogueira, F. M. S., Gross, E. K. U., Rubio, A., Eds.; *Fundamentals of Time-Dependent Density Functional Theory*; Springer: Berlin, 2012.

(15) Bloch, F. Bremsvermögen von Atomen mit Mehreren Elektronen. *Z. Phys.* **1933**, *81*, 363−376.

(16) Eguiluz, A.; Ying, S. C.; Quinn, J. J. Influence of the Electron Density Profile on Surface Plasmons in a Hydrodynamic Model. *Phys. Rev. B* **1975**, *11*, 2118−2121.

(17) Lunqvist, S., March, N. H., Eds.; *Theory of the Inhomogeneous Electron Gas*; Plenum: New York, 1983.

8948

dx.doi.org/10.1021/jp401887y | J. Phys. Chem. C 2013, 117, 8941−8949

(18) Ciraci, C.; Hill, R. T.; Mock, J. J.; Urzhumov, Y.; Ferná ndez-Domnguez, A. I.; Maier, S. A.; Pendry, J. B.; Chilkoti, A.; Smith, D. R. Probing the Ultimate Limits of Plasmonic Enhancement. *Science* **2012**, *337*, 1072−1074.

(19) Raza, S.; Stenger, N.; Kadkhodazadeh, S.; Fischer, S. V.; Kostesha, N.; Jauho, A.-P.; Burrows, A.; Wubs, M.; Mortensen, N. A. Blueshift of the Surface Plasmon Resonance in Silver Nanoparticles Studied with EELS. *Nanophotonics* **2013**, *2*, in press.

(20) Savage, K. J.; Hawkeye, W. M.; Esteban, R.; Borisov, A. G.; Aizpurua, J.; Baumberg, J. J. Revealing the Quantum Regime in Tunnelling Plasmonics. *Nature* **2012**, *491*, 574−577.

(21) Ruppin, R. Extinction Properties of Thin Metallic Nanowires. *Opt. Commun.* **2001**, *190*, 205−209.

(22) McMahon, J. M.; Gray, S. K.; Schatz, G. C. Nonlocal Optical Response of Metal Nanostructures with Arbitrary Shape. *Phys. Rev. Lett.* **2009**, *103*, 097403.

(23) McMahon, J. M.; Gray, S. K.; Schatz, G. C. Optical Properties of Nanowire Dimers with a Spatially Nonlocal Dielectric Function. *Nano Lett.* **2010**, *10*, 4373−3481.

(24) Villo-Pérez, I., Miskovic, Z. L., Arista, N. R. In Aldea, A., Bârsan, V., Eds.; *Trends in Nanophysics*; Springer: Berlin, 2010.

(25) Raza, S; Toscano, G.; Jauho, A.-P.; Wubs, M.; Mortensen, N. A. Unusual Resonances in Nanoplasmonic Structures Due to Nonlocal Response. *Phys. Rev. B* **2011**, *84*, 121412(R).

(26) David, C.; Garca de Abajo, F. J. Spatial Nonlocality in the Optical Response of Metal Nanoparticles. *J. Phys. Chem. C* **2011**, *115*, 19470−19475.

(27) Fernández-Domnguez, A. I.; Wiener, A.; Garca-Vidal, F. J.; Maier, S. A.; Pendry, J. B. Transformation-Optics Description of Nonlocal Effects in Plasmonic Nanostructures. *Phys. Rev. Lett.* **2012**, *108*, 106802.

(28) Boardman, A. D. *Electromagnetic Surface Modes*; Wiley: New York, 1982.

(29) Wiener, A.; Fernández-Domínguez, A. I.; Horsfield, A. P.; Pendry, J. B.; Maier, S. A. Nonlocal Effects in the Nanofocusing Performance of Plasmonic Tips. *Nano Lett.* **2012**, *12*, 3308−3314.

(30) Dobson, J. F.; Le, H. M. High-Frequency Hydrodynamics and Thomas-Fermi Theory. *J. Mol. Struct. (THEOCHEM)* **2000**, *501*, 327−338.

(31) Liebsch, A. *Electron Excitations at Metal Surfaces*, Plenum: New York, 1997.

(32) Liebsch, A. Surface Plasmon Dispersion of Ag. *Phys. Rev. Lett.* **1993**, *71*, 145−148.

(33) Serra, L.; Rubio, A. Core Polarization in the Optical Response of Metal Clusters: Generalized Time-Dependent Density-Functional Theory. *Phys. Rev. Lett.* **1997**, *78*, 1428−1431.

(34) Kim, J. S.; Chen, L.; Kesmodel, L. L.; Garca-González, P.; Liebsch, A. Surface Plasmon Dispersion of Cl/Ag(111). *Phys. Rev. B* **1997**, *56*, 4402−4405(R).

(35) Smogunov, A. N.; Kurkina, L. I.; Farberovich, O. V. Electronic Structure and Polarizability of Quantum Metallic Wires. *Phys. Solid State* **2000**, *42*, 18981907.

(36) Kreibig, U.; Genzel, L. Optical Absorption of Small Metallic Particles. *Surf. Sci.* **1985**, *156*, 678−700.

(37) COMSOL Multiphysics 3.5a, COMSOL AB, Stockholm.

(38) Toscano, G.; Raza, S.; Jauho, A.-P.; Mortensen, N. A.; Wubs, M. Modified Field Enhancement in Plasmonic Nanowire Dimers Due to Nonlocal Response. *Opt. Express* **2012**, *20*, 4176−4188.

(39) Hiremath, K. R.; Zschiedrich, L.; Schmidt, F. Numerical Solution of Nonlocal Hydrodynamic Drude Model for Arbitrary Shaped Nano-Plasmonic Structures using Nedelec Finite Elements. *J. Comput. Phys.* **2012**, *231*, 5890−5896.

(40) Marques, M. A. L.; Castro, A.; Bertsch, G. F.; Rubio, A. Octopus: a First-Principles Tool for Excited Electron-Ion Dynamics. *Comput. Phys. Commun.* **2003**, *151*, 60−78.

(41) Castro, A.; Appel, H.; Oliveira, M.; Rozzi, C. A.; Andrade, X.; Lorenzen, F.; Marques, M. A. L.; Gross, E.; Rubio, A. Octopus: a Tool for the Application of Time-Dependent Density Functional Theory. *Phys. Status Solidi B* **2006**, *243*, 2465−2488.

(42) Andrade, X.; Alberdi-Rodriguez, J.; Strubbe, D. A.; Oliveira, M. J. T.; Nogueira, F.; Castro, A.; Muguerza, J.; Arruabarrena, A.; Louie, S. G.; Aspuru-Guzik, A.; et al. Time-Dependent Density-Functional Theory in Massively Parallel Computer Architectures: the Octopus Project. *J. Phys.: Condens. Matter* **2012**, *24*, 233202.

(43) Ekardt, W. Dynamical Polarizability of Small Metal Particles: Self-Consistent Spherical Jellium Background Model. *Phys. Rev. Lett.* **1984**, *52*, 19251928.

(44) Townsend, E.; Bryant, G. W. Plasmonic Properties of Metallic Nanoparticles: The Effects of Size Quantization. *Nano Lett.* **2011**, *12*, 429−434.

(45) Bennet, A. J. Influence of the Electron Charge Distribution on Surface-Plasmon Dispersion. *Phys. Rev. B* **1970**, *1*, 203−207.

(46) Tsuei, K. D.; Plummer, E. W.; Liebsch, A.; Phelke, E.; Kempa, K.; Bakshi, P. The Normal Modes at the Surface of Simple Metals. *Surf. Sci.* **1991**, *247*, 302−326.

(47) Anderegg, M.; Feuerbacher, B.; Fitton, B. Optically Excited Longitudinal Plasmons in Potassium. *Phys. Rev. Lett.* **1971**, *27*, 1565−1686.

(48) Romero, I.; Aizpurua, J.; Bryant, G. W.; Garca de Abajo, F. J. Plasmons in Nearly Touching Metallic Nanoparticles: Singular Response in the Limit of Touching Dimers. *Opt. Express* **2006**, *14*, 9988−9999.

(49) Zuolaga, J.; Prodan, E.; Nordlander, P. Quantum Description of the Plasmon Resonances of a Nanoparticle Dimer. *Nano Lett.* **2009**, *9*, 887−891.

(50) Marinica, D. C.; Kazansky, A. K.; Nordlander, P.; Aizpurua, J.; Borisov, A. G. Quantum Plasmonics: Nonlinear Effects in the Field Enhancement of a Plasmonic Nanoparticle Dimer. *Nano Lett.* **2012**, *12*, 1333−1339.

(51) Esteban, R.; Borisov, A. G.; Nordlander, P.; Aizpurua, J. Bridging Quantum and Classical Plasmonics with a Quantum-Corrected Model. *Nat. Commun.* **2012**, *3*, 825.

(52) Prodan, E.; Radloff, C.; Halas, N. J.; Nordlander, P. A Hybridization Model for the Plasmon Response of Complex Nanostructures. *Science* **2003**, *302*, 419−422.

(53) Dong, T.; Ma, X.; Mittra, R. Optical Response in Subnanometer Gaps Due to Nonlocal Response and Quantum Tunneling. *Appl. Phys. Lett.* **2012**, *101*, 233111.

(54) Ozturk, Z. F.; Xiao, S.; Yan, M.; Wubs, M.; Jauho, A.-P.; Mortensen, N. A. Field Enhancement at Metallic Interfaces Due to Quantum Confinement. *J. Nanophotonics* **2011**, *5*, 051602.

(55) Schwartz, C.; Schaich, W. L. Hydrodynamic Models of Surface Plasmons. *Phys. Rev. B* **1982**, *26*, 7008−7011.